Atmospheric Environment 190 (2018) 87–98

Contents lists available at ScienceDirect

Atmospheric Environment

journal homepage: www.elsevier.com/locate/atmosenv

Characteristics and source apportionment of black carbon in the Helsinki metropolitan area, Finland

Aku Helin[a,*], Jarkko V. Niemi[b], Aki Virkkula[a], Liisa Pirjola[c], Kimmo Teinilä[a], John Backman[a], Minna Aurela[a], Sanna Saarikoski[a], Topi Rönkkö[d], Eija Asmi[a], Hilkka Timonen[a]

[a] Atmospheric Composition Research, Finnish Meteorological Institute, P.O. Box 503, FI-00101, Helsinki, Finland
[b] Helsinki Region Environmental Services Authority, P.O. Box 100, FI-00066 HSY, Helsinki, Finland
[c] Department of Technology, Metropolia University of Applied Sciences, P.O. Box 4021, FI-00180, Helsinki, Finland
[d] Aerosol Physics, Faculty of Natural Sciences, Tampere University of Technology, P.O. Box 692, FI-33720, Tampere, Finland

ARTICLE INFO

Keywords:
Aethalometer
Black carbon
Absorption Ångström exponent
Fossil fuel
Biomass burning

ABSTRACT

Black carbon is emitted from the incomplete combustion of carbonaceous fuels and will detrimentally affect air quality, climate and human health. In this study, equivalent black carbon (eBC) concentrations were measured by using an aethalometer (AE33) at three different locations in the Helsinki metropolitan area, Finland from October 2015 to May 2017. One sampling site was located in an urban street canyon (SC, sampling period 18 months) and two of the sampling sites were located in suburban detached house (DH) areas (DH1, 13 months and DH2, 5 months). Based on the campaign averages, the eBC concentration levels were higher at the street canyon site (1690 ± 1520 ng/m^3) than at the residential detached house areas (DH1 = 880 ± 1500 ng/m^3 and DH2 = 1040 ± 2130 ng/m^3). The contribution of eBC from fossil fuel (BC_{FF}) and wood burning (BC_{WB}) were estimated based on the spectral dependence of light absorption of different sources. The spectral behavior is described using absorption Ångström exponent (α) values for both fossil fuel (α_{FF}) and wood burning (α_{WB}) that were determined using concurrent wood burning tracer (levoglucosan) measurements. Based on the source apportionment, the contribution of BC_{WB} to eBC was clearly higher at the detached house area sites DH1 (41 ± 14%) and DH2 (46 ± 15%) than at the urban street canyon site (15 ± 14%). A distinct seasonal dependency was observed in the eBC concentration levels at the detached house areas. The highest concentrations were detected during the cold seasons due to residential wood combustion. On the opposite, at the SC site, the concentration levels of eBC were rather constant throughout the campaign, being dominated by the BC_{FF} emissions from close-by vehicular traffic. Substantial temporal and spatial variability in eBC concentrations and sources were observed within the Helsinki metropolitan area. eBC is shown to be closely tied to the characteristics of the measurement site, season, meteorological conditions and the time of the day.

1. Introduction

Light-absorbing carbonaceous (LAC) aerosols are ubiquitous in the atmosphere. They are emitted and formed from e.g. the combustion processes of fossil fuel and biomass, biogenic sources and via heterogeneous/multiphase reactions (Andreae and Gelencsér, 2006; Bond et al., 2013; Laskin et al., 2015). "Black carbon" (BC) belongs to this group of LAC compounds, and it is considered to be the most important light absorbing aerosol component in the atmosphere due to the positive radiative forcing it imposes on the climate (IPCC, 2014). In addition to various climate impacts, BC deposited on snow may lead to a reduction of snow albedo and BC has adverse effects on public health (Hansen and Nazarenko, 2004; WHO, 2012; Bond et al., 2013). BC sources in urban areas are characteristically dominated by combustion processes, typically from anthropogenic sources, such as transportation, industry and residential combustion (Bond et al., 2013; Klimont et al., 2017). It has been estimated that, globally, 24% and 60% of anthropogenic BC emissions are from transport and residential combustion sources, respectively (Klimont et al., 2017). However, there are substantial spatial and temporal variabilities in the BC emissions. For example in Western Europe, the contribution of BC from transport and residential biomass burning sources was estimated to be 62% and 28%, respectively (Klimont et al., 2017). Whereas there is a declining trend in BC emissions from vehicular traffic due to technology advancements

* Corresponding author.
E-mail address: aku.helin@fmi.fi (A. Helin).

https://doi.org/10.1016/j.atmosenv.2018.07.022
Received 12 January 2018; Received in revised form 6 July 2018; Accepted 10 July 2018
Available online 11 July 2018

and legislation, the emissions from residential combustion are not currently regulated in most European countries (Briggs and Long, 2016; Klimont et al., 2017). Therefore, there has been growing interest to conduct BC source apportionment studies at different locations.

Black carbon concentrations have been determined using a variety of methods, such as light absorption based instruments measuring equivalent black carbon (eBC), thermal pyrolysis techniques measuring elemental carbon (EC) and thermal radiation techniques measuring refractory black carbon (rBC) (Pöschl, 2003; Bond et al., 2013; Petzold et al., 2013). Many of these measurement techniques can be applied for BC source apportionment studies (Briggs and Long, 2016). The spectral dependency between emissions from fossil fuel and biomass burning sources has made optical determination methods utilizing multi-wavelength light absorption instruments an interesting alternative to apportion eBC from these source categories. For example, the aethalometer, which measures aerosol light absorption in the wavelength range of 370–950 nm, can be used to estimate the contribution of eBC from the two sources (Sandradewi et al., 2008b; Herich et al., 2011; Wang et al., 2011a, 2011b). When compared to thermal methods used to quantify EC and its sources, optical methods usually provide superior time resolution. Thermal methods typically utilize separate filter sampling, and the source apportionment conducted by using radiocarbon (^{14}C) measurements are particularly time-consuming to conduct. In addition, light absorption based instruments are typically inexpensive, portable and relatively easy to use compared with devices measuring EC and rBC.

The eBC source apportionment method used with the aethalometer, also known as the Aethalometer model (Sandradewi et al., 2008a, 2008b; Herich et al., 2011), capitalizes on the different spectral dependencies of fossil fuel and biomass burning originating LAC aerosols. Overall, eBC is a strong light absorber over the whole visible wavelength region. In emission from fossil fuel sources, eBC is expected to be the dominant LAC component absorbing in the long visible and near infrared (IR) wavelengths (~600–950 nm) (Kirchstetter et al., 2004; Sandradewi et al., 2008a, 2008b). However, in emissions from biomass burning there are also other LAC compounds present (e.g. organic brown carbon constituents) which contribute significantly to the light absorption close to the near ultraviolet (UV) and lower visible wavelengths (~300–500 nm) (Kirchstetter et al., 2004; Sandradewi et al., 2008b; Laskin et al., 2015). Based on these observations, in the Aethalometer model the absorption near-UV and near-IR regions are considered to be indicative of eBC from wood burning (BC_{WB}) and fossil fuel (BC_{FF}) sources, respectively. In its simplest form, the model is based on the assumption that emissions from fossil fuel and biomass burning sources follow spectral dependencies of λ^{-1} and λ^{-2}, respectively. These exponents are called absorption Ångström exponents (α), descriptive of the spectral dependence of light absorption.

Following this reasoning, the fundamental principle of the Aethalometer model is based on the preselection of suitable α values for fossil fuel (α_{FF}) and biomass burning (α_{WB}) (Sandradewi et al., 2008b; Zotter et al., 2017). Consequently, one of the most significant uncertainties in the model is related to assigning fixed site-specific α_{FF} and α_{WB} values (Healy et al., 2017; Zotter et al., 2017). Different α values have been used depending on the sampling site and the selected wavelength pairs used in the model, but α_{FF} close to 1 and α_{WB} in the range of 1.6–2.2 are most commonly found in the literature (Sandradewi et al., 2008b; Herich et al., 2011; Sciare et al., 2011; Fuller et al., 2014; Liu et al., 2014; Becerril-Valle et al., 2017; Titos et al., 2017; Zotter et al., 2017). Overall, there is good consensus that α values are approximately in the range of 0.8–1.2 for fossil fuel, but the α values for biomass burning can vary significantly depending on e.g. the type of fuel combusted and combustion conditions (Kirchstetter et al., 2004; Harrison et al., 2013; Saleh et al., 2013; Garg et al., 2015; Martinsson et al., 2015). Furthermore, α values are affected by the BC particle core size, the chemical composition of the surrounding coating and coating thickness (Gyawali et al., 2009; Lack and Cappa, 2010; Lack and Langridge, 2013). All of these factors increase the uncertainty of aethalometer based source apportionment. Nevertheless, multiple studies have demonstrated the applicability of the Aethalometer model being appropriate for estimating the different sources of eBC (Herich et al., 2011; Crilley et al., 2015; Becerril-Valle et al., 2017; Healy et al., 2017; Zotter et al., 2017).

There are limited number of long-term studies covering the source apportionment of eBC in northern Europe, and the contribution of wood burning on eBC ambient levels has not yet been thoroughly estimated (Elser et al., 2016; Martinsson et al., 2017). In Scandinavia, and especially in Finland, wood burning has long traditions for heating houses and saunas. Experimental studies and emission inventories have indicated that sauna stoves emit relatively large amounts of BC, which, among other residential wood combustion, can contribute significantly to Finland's total BC emissions (Tissari et al., 2007; Hienola et al., 2013; Savolahti et al., 2016). As there is a demand for studies estimating eBC sources at northern regions for better evaluating the dispersion and emission strengths, our aim in this study was to investigate the variation of eBC at three different locations inside the Helsinki metropolitan area in Finland. One of the sites was located in an urban street canyon whereas two of the sites were situated in suburban detached house areas. These sites represent characteristically different environments within a metropolitan area. The Aethalometer model was utilized to evaluate the relative contributions of BC_{FF} and BC_{WB} at these sites.

2. Experimental section

2.1. Measurement sites

Measurements were conducted at three different sites in the Helsinki metropolitan area (HMA). The HMA consists of the cities of Helsinki, Vantaa, Espoo and Kauniainen with a total population of approximately 1.1 million. General information about the characteristics of the HMA can be found elsewhere (Saarnio et al., 2012; Hellén et al., 2017; Kaski et al., 2017). In brief, however, the contribution of different emission source categories to $PM_{2.5}$ in the HMA in 2016 were estimated to be as follows: 37% from small-scale wood combustion, 36% from energy production in large power and heating plants, 23% from vehicular traffic and the rest (4%) from a variety of sources (e.g. industry and harbors) (Kaski et al., 2017). District heating is the primarily used heating method in the HMA. The majority of the fuel used for the energy production within the HMA in 2016 was coal (58%) and natural gas (33%). In the detached house areas ~90% of houses have a fireplace and wood burning is used for partial heating, warming of sauna stoves and decorative burning.

In this study, one of the sampling sites was located in a street canyon near the city center on the street Mäkelänkatu in Helsinki. The other two sampling sites were located in suburban detached house areas (Lintuvaara, Espoo and Rekola, Vantaa). Hereafter, the sampling sites are referred to as street canyon (SC, Mäkelänkatu), detached house area 1 (DH1, Lintuvaara) and detached house area 2 (DH2, Rekola). The street canyon station was on the curb side of a busy traffic six-lane street, where the average traffic density was 28000 vehicles/day (11% heavy duty vehicles). The traffic volumes were substantially lower at the detached house areas. At DH1, the distance to the busiest nearby street was 400 m, where the traffic volume was 4200 vehicles/day. At DH2, the traffic volume of the nearest busy street was 5200 vehicles/day at the distance of 105 m. All the sampling locations were within a radius of ~18 km of each other.

2.2. Aethalometer measurements and source apportionment

A dual-spot aethalometer (AE33, Magee Scientific) was used to measure the aerosol light absorption and corresponding eBC mass concentration at seven different wavelengths (370–950 nm) (Hansen et al., 1984; Drinovec et al., 2015). The flow rate was set to 5 L/min, the

inlet cut-off size was 1 μm (sharp cut cyclone, BGI model SCC1.197) and the measurement time resolution was set to 1 min. The filter tape used was TFE-coated glass fiber filters (no. M8020). The multiple scattering enhancement factor C was set to 1.57 (Drinovec et al., 2015). Two AE33 instruments were used to sample at the three different locations with identical measurement settings. The sampling inlet height was 4 m above the ground at all sites. One AE33 was measuring continuously at the urban SC site from October 2015 to May 2017 during the whole period. The other AE33 was first measuring at the suburban DH1 site from December 2015 to December 2016 and then at the DH2 site from January 2017 to May 2017. In addition, there was a short inter-comparison period in late winter 2016, during which both instruments were sampling through the same inlet at the street canyon location (for results see Supplementary Information SI1, Table S1 and Fig. S1).

The recently developed AE33 model provides aerosol light absorption coefficient ($b_{abs}(\lambda)$) and eBC concentration in real-time that have been compensated for filter loading artifacts and tape advancement error (Drinovec et al., 2015). The default mass absorption cross-section (MAC) values given by the manufacturer were used in this study (Drinovec et al., 2015). The eBC mass concentration is here reported at a wavelength of 880 nm. In order to estimate the contribution of wood burning and fossil fuel to eBC, equations (1)–(6) were used in calculations by following the source apportionment method referred as the Aethalometer model (Sandradewi et al., 2008b). Wavelengths 470 nm and 950 nm were used for the source apportionment (equations (1)–(3)), and to calculate the biomass burning percentage (BB%, equation (4)) which was then used to calculate the BC_{FF} and BC_{WB} concentrations (equations (5) and (6)) by following the procedure given in the AE33 manual (Magee Scientific, 2016). In all calculations, the wavelength of 880 nm was used to report the mass concentrations of eBC, BC_{FF} and BC_{WB}. The absorption Ångström exponent (α) was calculated by using equation (7).

$$\frac{b_{abs}(470\ \mathrm{nm})_{FF}}{b_{abs}(950\ \mathrm{nm})_{FF}} = \left(\frac{470}{950}\right)^{-\alpha_{FF}} \quad (1)$$

$$\frac{b_{abs}(470\ \mathrm{nm})_{WB}}{b_{abs}(950\ \mathrm{nm})_{WB}} = \left(\frac{470}{950}\right)^{-\alpha_{WB}} \quad (2)$$

$$b_{abs}(\lambda) = b_{abs}(\lambda)_{FF} + b_{abs}(\lambda)_{WB} \quad (3)$$

$$\mathrm{BB}(\%) = \frac{b_{abs}(950\ \mathrm{nm})_{WB}}{b_{abs}(950\ \mathrm{nm})} \quad (4)$$

$$BC_{WB} = \mathrm{BB}{*}\mathrm{eBC} \quad (5)$$

$$BC_{FF} = (1 - \mathrm{BB}){*}\mathrm{eBC} \quad (6)$$

$$\alpha = -\frac{\ln(b_{abs}(470\ \mathrm{nm})/b_{abs}(950\ \mathrm{nm}))}{\ln(470/950)} \quad (7)$$

Previous studies have typically either determined the α_{FF} and α_{WB} values by using auxiliary measurements (e.g. EC/OC and ^{14}C measurements) (Sandradewi et al., 2008b; Zotter et al., 2017) or by referring to commonly used values in the literature (Elser et al., 2016; Healy et al., 2017; Martinsson et al., 2017; Rajesh and Ramachandran, 2017; Zhu et al., 2017; Jereb et al., 2018). In addition, recent studies have used levoglucosan measurements together with the Aethalometer model for estimating site specific α_{FF} and α_{WB} values (Fuller et al., 2014; Titos et al., 2017). Levoglucosan is commonly used as a tracer for biomass burning derived aerosols (Simoneit et al., 1999; Yttri et al., 2005; Puxbaum et al., 2007; Saarikoski et al., 2008b; Saarnio et al., 2012; Hellén et al., 2017). We applied this procedure utilizing levoglucosan measurements together with the Aethalometer model to estimate the site specific α values in the HMA area. In principle, levoglucosan should correlate with BC_{WB} and the intercept of the linear regression equation should be close to zero, assuming that both tracers experience similar atmospheric removal rates (Fuller et al., 2014; Titos et al., 2017). In order to examine which α_{FF} and α_{WB} combinations yields intercepts closest to zero, the α_{FF} was varied in the range of 0.8–1.2 and the α_{WB} in the range of 1.4–2.2. These α ranges cover commonly used values in the literature. Collectively, each possible α pair was evaluated by plotting levoglucosan concentration as a function of the corresponding BC_{WB} concentration and linear regression analysis was applied. For clarity, the equation used to calculate all the possible BC_{WB} concentrations is shown in equation (8) (derived from equations (1)–(5)). Further description of the procedure and results are given in Section 3.2.

$$BC_{WB} = \frac{\left(\frac{b_{abs}(470\ nm) - b_{abs}(950\ nm) * \left(\frac{470}{950}\right)^{-\alpha_{FF}}}{\left(\frac{470}{950}\right)^{-\alpha_{WB}} - \left(\frac{470}{950}\right)^{-\alpha_{FF}}}\right)}{b_{abs}(950\ nm)} * \mathrm{eBC} \quad (8)$$

2.3. Filter sampling measurements

PM_{10} samples used for levoglucosan analysis were collected at the street canyon and detached house area (DH1) sites. The sampling started at midnight and the sampling time and volume were 24 h and ~55 m^3, respectively. Samples were collected every third day and occasionally each day. At the SC site, the sampling period was from October 2015 to October 2016 and a total of 146 filter samples were analyzed. The sampling period was from December 2015 to May 2016 at the DH1 site and a total of 76 filter samples were analyzed. The filter samples were extracted prior to high-performance anion-exchange chromatographic-mass spectrometric analysis by following the analytical method presented in Saarnio et al. (2010), with the exception of using methyl-β-D-arabinopyranoside (purity 99%, Aldrich Chemical Co., USA) as an internal standard (Saarnio et al., 2013). Levoglucosan results from these filter samples were used in the estimation of site specific α values.

In addition, a total of 32 of PM_1 samples were collected during May–August 2016 at the street canyon site, and EC/OC concentrations were determined by applying the EUSAAR_2 procedure given in Cavalli et al. (2010). The EC results were used to estimate the site specific MAC values for the SC site, and the results from these are presented in the Supplementary Information (SI2, Table S2). These derived MAC values were not used to compute the eBC concentration levels presented in this study, however, we report these in the SI as additional information for future studies to benefit and compare to.

2.4. Auxiliary measurements

Auxiliary measurements of different parameters were obtained as part of the Helsinki Region Environmental Services Authority measuring network (Kaski et al., 2017). Air quality parameters (NO_x and $PM_{2.5}$ concentration) were monitored with 1-min time resolution at eBC measurement sites throughout the corresponding sampling periods. Furthermore, meteorological parameters (air temperature, wind speed and direction) were measured on-site or close-by to the measurement stations. These auxiliary parameters were mainly used in correlation studies. In addition, simultaneous multi-angle absorption photometer (MAAP, model 5012, Thermo Fisher Scientific) (Petzold and Schönlinner, 2004) eBC mass concentration measurements were conducted at the SC and DH1 sites. The intercomparison of the aethalometer and MAAP performance in terms of measured eBC mass concentration is shown in the supplementary material (SI3, Fig. S2).

2.5. Data processing and statistical analyses

All the available air quality data had a time resolution of 1-min. These data were hourly-averaged and particulate components were calculated to local ambient conditions and gaseous components to standardized conditions (T = 293.15 K and p = 101.3 kPa) by following EU guidelines. A criterion of 75% data coverage was set for the

hourly averaged and further in daily averaged data. The monthly averages were derived from the hourly averaged data and the data coverage was typically higher than 95%, except during February at the DH1 site the aethalometer data coverage was 65%.

In order to study the differences between the urban traffic site and suburban residential areas, we chose to focus explicitly on the SC and DH1 data, which had the longest overlapping collection periods covering seasonality (Section 2.2.). Unfortunately, during autumn 2016 at the street canyon site, two months of source apportionment data had to be rejected due to AE33 filter batch change. The new filter tape batch (no. M8050) did not affect the near-IR wavelength absorption coefficient results, however, the near-UV region results were compromised according to the manufacturer's announcement. The aethalometer eBC data validity from this time period was additionally checked against MAAP data, and no anomalies were observed (data not shown). Due to these limitations in concurrent data availability, our study focuses on resolving the differences between the extremity seasons, namely winter and summer, in BC_{FF} and BC_{WB} results. In late autumn 2016 the filter batch was replaced with the old one (no. M8020) at the SC site, allowing the source apportionment for the rest of the time. The intercomparison between the different sites was based on concurrent sampling periods.

All statistical elaborations were obtained by using statistical software R (R Core Team, 2017). Daily averaged values were used in correlation analysis between different meteorological variables and air quality parameters with eBC concentration. In the following sections, all correlations shown correspond to statistical significance level of $p \leq 0.001$. Bivariate polar plots of BC_{FF} and BC_{WB} hourly mean concentration levels in different wind conditions were obtained by using the openair R package (Carslaw and Ropkins, 2012, 2017; Carslaw and Beevers, 2013). Wind data used in these were taken from masts at heights of 53 m (Pasila, Helsinki) and 10 m (Ämmässuo, Espoo) above ground level, which were representative of the prevailing conditions above the SC and DH1 sites, respectively.

3. Results and discussion

3.1. General characteristics of eBC concentrations and sources

Based on the overall campaign averages, the eBC concentrations were the highest at the street canyon site (Table 1). There were also clear differences in the seasonal variations of eBC concentration levels at the three sampling sites (Fig. 1). At the SC site, eBC concentration levels were relatively constant throughout the campaign and no distinct seasonal variation was observed. On the contrary, at the detached house areas eBC concentrations were strongly elevated in winter, rising close to the levels observed at the SC site (Fig. 1). During winter (December 2015–February 2016) the average ± standard deviation concentrations of eBC were 1670 ± 1390 ng/m^3 and 1520 ± 2570 ng/m^3 at the SC and DH1 sites, respectively. During summer (June–August 2016), the eBC concentrations at these sites were on average 1940 ± 1530 ng/m^3 (SC) and 450 ± 420 ng/m^3 (DH1). Similarly, during the beginning of 2017 (January–February), the eBC concentrations were on average 1690 ± 1460 ng/m^3 and 1560 ± 3090 ng/m^3 at the SC and DH2 sites, respectively. During the intermediate season (March–May 2017), the eBC concentrations were on average 1380 ± 1160 ng/m^3 at SC and 730 ± 1150 ng/m^3 at DH2. In general, the measured eBC concentration levels in the HMA were similar to or lower than those detected in other European locations (Reche et al., 2011; Singh et al., 2018). For example in recent long-term studies, the average eBC concentration at different urban sites in Europe were ~1200–1400 ng/m^3 and ~1210–3700 ng/m^3 in $PM_{2.5}$ and PM_{10} samples, respectively (Crilley et al., 2015; Birmili et al., 2016; Becerril-Valle et al., 2017; Diapouli et al., 2017). In addition, our results are in agreement with previous studies conducted in the HMA (Pakkanen et al., 2000; Järvi et al., 2008). Overall, the eBC concentration levels measured at the HMA were roughly 2- to 10-fold higher than in other remote and rural locations in Finland (Hyvärinen et al., 2011).

Moderate negative correlation was observed between air temperature and eBC concentration at the suburban sites DH1 (Pearson's $R = -0.53$) and DH2 ($R = -0.48$), whereas at the urban SC site the correlation was negligible ($R = 0.14$). During the cold season, additional wood heating is common in Finland and the observed increase in eBC concentration levels at the detached house areas (Fig. 1) could be explained by increased emissions from residential wood combustion (Savolahti et al., 2016; Pirjola et al., 2017). At the busy traffic SC site, the eBC concentration variation was less affected by temperature variation and additional heating, since the surrounding block houses in the city center do not have fireplaces (Hellén et al., 2017). The eBC concentration levels were relatively stable throughout the whole sampling period at SC, indicating a relative constant sources of eBC at this site, e.g. vehicular traffic (Reche et al., 2011; Singh et al., 2018). The strongest correlation between NO_x with eBC concentration was observed at SC ($R = 0.87$), although the correlation was also significant at the DH1 ($R = 0.85$) and DH2 ($R = 0.82$) sites. Consequently, considering that traffic is a major source of NO_x this suggests that the eBC concentrations are affected by dispersed traffic emissions at all sites. Residential heating can contribute locally to NO_x and eBC concentrations at the DH1 and DH2 sites. However, the NO_x levels were substantially lower at the detached house areas than at the street canyon site (Table 1). Furthermore, previous studies have observed a rapid decrease in BC concentrations when the distance from the road increases (Zhu et al., 2002; Massoli et al., 2012), e.g. at HMA highway areas, the eBC levels half-decay distance was estimated to be ~33 m (Enroth et al., 2016). Thus, assumingly the local traffic sources are mainly affecting the eBC levels at SC, whereas at the detached house areas, the traffic emissions are diminished close to background levels (see Section 2.1 traffic volumes and road distance).

The monthly variation pattern of absorption Ångström exponent (α) at the three sites was similar (Fig. 1). The highest α values were observed during the cold season and the lowest during the summer; a trend which has been seen in previous studies as well (Herich et al., 2011; Crilley et al., 2015; Ran et al., 2016; Martinsson et al., 2017; Titos et al., 2017). The median α values were constantly higher at the detached house areas than at the street canyon site (Fig. 1). In general, high α values are indicative of biomass burning and low α values of fossil fuel derived eBC sources (Kirchstetter et al., 2004; Sandradewi et al., 2008a, 2008b). Thus, this supports the hypothesis that the highest eBC levels observed at the detached house areas during cold seasons are strongly affected by wood combustion sources. Furthermore, considering that the α values were higher at the DH1 than at the SC throughout the sampling period highlights the differences in eBC sources between these sites, namely wood combustion and fossil fuel

Table 1
Average (± standard deviation) concentration levels of different variables at the three sampling sites (SC = street canyon and DH = detached house area) calculated based on the corresponding entire sampling periods.

Variable	Urban SC (Oct 2015–May 2017)	Suburban DH1 (Dec 2015–Dec 2016)	Suburban DH2 (Jan 2017–May 2017)
eBC (ng/m^3)	1690 ± 1520	880 ± 1500	1040 ± 2130
BC_{FF} (ng/m^3)	1570 ± 1480	489 ± 770	510 ± 930
BC_{WB} (ng/m^3)	140 ± 210	390 ± 800	530 ± 1260
BB (%)	15 ± 14	41 ± 14	46 ± 15
α	1.16 ± 0.09	1.25 ± 0.11	1.29 ± 0.11
NO_x (μg/m^3)	93 ± 95	15 ± 28	16 ± 21
$PM_{2.5}$ (μg/m^3)	7.8 ± 5.1	7.3 ± 6.9	5.8 ± 4.8
Levoglucosan (ng/m^3)[a]	40 ± 50	94 ± 130	n.a.

[a] SC: Oct 2015–Oct 2016 and DH1: Dec 2015–May 2016.

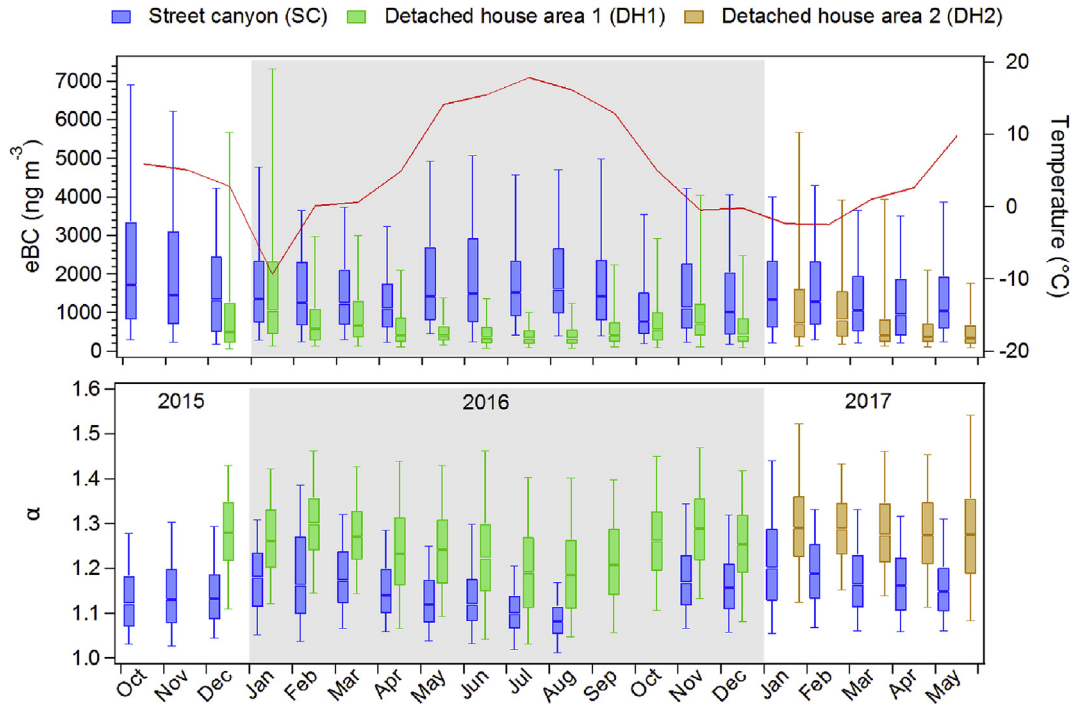

Fig. 1. Monthly variation of eBC concentration (upper panel), average air temperature (red line, upper panel) and absorption Ångström exponent (lower panel) at the three sampling sites in the HMA. The box edges show the 25th to 75th percentile range, the vertical line shows the 50th percentile whereas the whiskers indicate the 5th to 95th percentile range. The shaded grey background area represents year 2016. (For interpretation of the references to color in this figure legend, the reader is referred to the Web version of this article.)

sources contribution. This is also supported by the measured levoglucosan concentration levels (Fig. S3; Table 1), which were on average approximately 2-fold higher at the DH1 (102 ± 138 ng/m^3) than at the SC (51 ± 60 ng/m^3), when considering the overlapping sampling periods (n = 65 samples). In addition, the observed correlation between levoglucosan with eBC concentration was more evident at the DH1 (R = 0.95) than at the SC (R = 0.32), further highlighting the differences between these sites.

3.2. Estimation of the site specific α_{FF} and α_{WB} values

In order to study the contribution of fossil fuel and wood burning derived eBC, the site specific α_{FF} and α_{WB} values were estimated. The site specific α values were determined in two steps by 1) utilizing concurrent levoglucosan measurements and by 2) evaluating the most plausible diurnal cycles of the resulting BC_{FF} and BC_{WB} concentrations.

Concurrent levoglucosan measurements were utilized to estimate the optimal α values (Section 2.2.). The demonstration of the linear fitting of levoglucosan concentrations between calculated BC_{WB} concentrations by using the far extreme α value combinations are presented in Fig. 2. These plots illustrate how the changing α values affect the BC_{WB} results and levoglucosan intercept in practice. The overall results are shown in Fig. S4, where the linear regression equation intercept of levoglucosan is plotted based on all different α_{FF} and α_{WB} combinations. In addition, correlation between levoglucosan with BC_{WB} is illustrated in Fig. S4. At the SC site, the intercept was evidently closest to zero at α_{FF} = 1.10, whereas at the DH1 the intercept was closest to zero at $\alpha_{FF} \approx$ 0.91–0.97 (Fig. S4). As a compromise, the α_{FF} value of 0.95 was selected for DH1. These derived optimal α_{FF} seemed to be reasonable as demonstrated in SI4 and Fig. S5. Considering the uncertainties, the corresponding α_{FF} values become 1.10 ± 0.05 at SC and 0.95 ± 0.15 at DH1, demonstrating the higher variability at the DH1 site. A plausible explanation are the mixed emission sources at the detached house area influenced by seasonality as discussed later on. The correlations between BC_{WB} and levoglucosan obtained by using the optimal α_{FF} values at SC and DH1 were R = 0.89 and R = 0.95, respectively (α_{WB} range 1.4–2.2, Fig. S4). The effect of α_{WB} within a fixed α_{FF} was not that evident (Fig. S4), as was also previously observed in other studies (Fuller et al., 2014; Titos et al., 2017), thus these levoglucosan intercept results cannot be explicitly used to determine the optimal α_{WB} values.

The wide range of α_{WB} values (1.4–2.2) used in these experiments somewhat complicates the possible differences in assessing the source contributions of BC_{WB} and BC_{FF} (SI4, Fig. S5). In the literature, fixed values of α_{FF} and α_{WB} are typically used in source apportionment studies for simplicity (Herich et al., 2011; Liu et al., 2014; Crilley et al., 2015; Elser et al., 2016; Healy et al., 2017; Martinsson et al., 2017; Petit et al., 2017; Rajesh and Ramachandran, 2017; Zotter et al., 2017). To find a single representative α_{WB} value for both sites, diurnal cycles of BC_{FF} and BC_{WB} during the winter and summer seasons were plotted at both locations (Fig. 3). The range of BC_{FF} and BC_{WB} concentrations are illustrated in Fig. 3 when using the α_{WB} range 1.4–2.2. Note that in the diurnal cycle plots, the far extremes represent the variation: when the BC_{WB} is at its highest (using α_{WB} = 1.4), the BC_{FF} is at its lowest and vice versa. The diurnal cycles were plotted in order to find most plausible α_{WB} value yielding reasonable daily cycles. We had two preliminary hypothesis, which are based on the previous source apportionment studies and on the characteristics of the sampling sites. First, during summer and morning rush hour the contribution of BC_{WB} should be negligible at the busy traffic street canyon site (Järvi et al., 2008; Saarnio et al., 2013). Second, at the detached house area during winter the BC_{WB} contribution is assumed more significant during evenings due to residential heating by burning wood (Saarnio et al., 2012; Aurela et al., 2015; Hellén et al., 2017).

As can be seen in Fig. 3a and b, the effect of different α_{WB} plays a relatively minor role at the street canyon site. The contribution of BC_{FF} is evident at this site despite of the selected α_{WB}. However, with the lowest α_{WB} values there is an artificial peak in BC_{WB} concentration during summer morning rush hour at SC (Fig. 3b). In contrast, at the suburban DH1 site, the choice of α_{WB} has more impact on the results

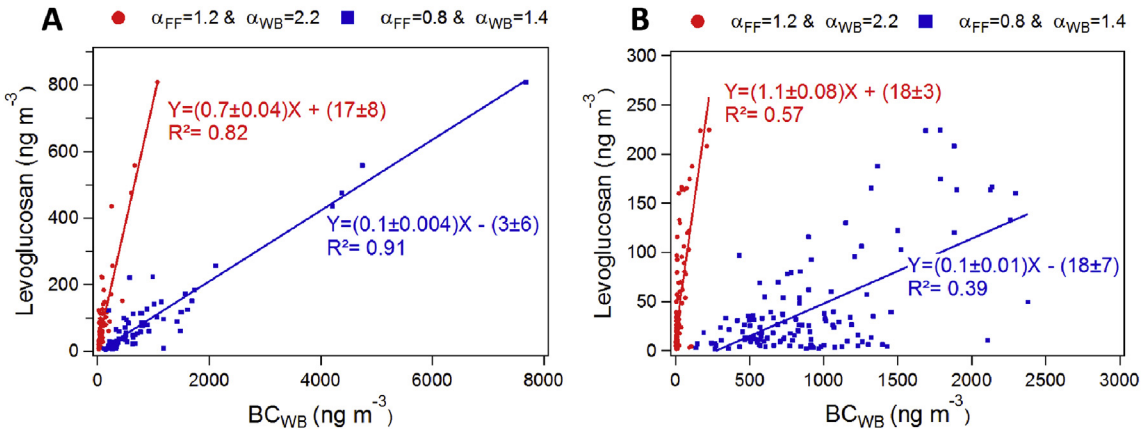

Fig. 2. Levoglucosan as a function of calculated BC_{WB} concentration based on the far extreme α value combinations at a) detached house area 1 and b) street canyon. The linear regression analysis results are embedded in the plots. Notice the difference in axis scales.

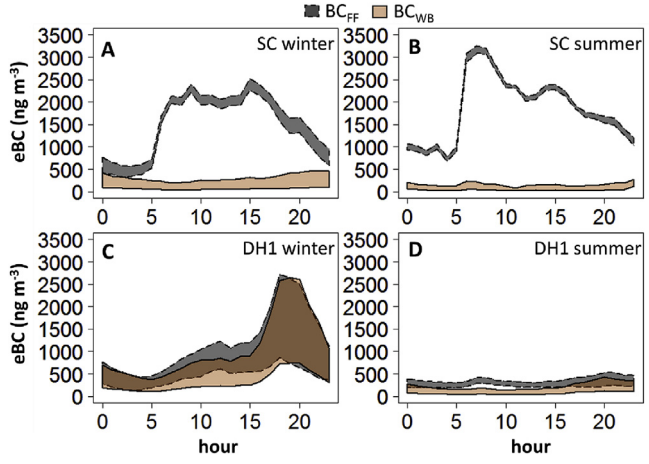

Fig. 3. Diurnal cycles of BC_{FF} and BC_{WB} concentrations at a) street canyon during winter b) street canyon during summer c) detached house area 1 during winter and d) detached house area 1 during summer. The concentration ranges cover extremes calculated using α_{WB} = 1.4–2.2 with fixed site specific α_{FF} values (SC: α_{FF} = 1.10 and DH1: α_{FF} = 0.95). In the plots, when the BC_{WB} is at its highest (α_{WB} = 1.4), the BC_{FF} is at its lowest and vice versa. The overlapping area is visualized as the darker brown color. (For interpretation of the references to color in this figure legend, the reader is referred to the Web version of this article.)

(Fig. 3c and d). When using α_{WB} = 1.4, the BC_{WB} is much higher than the BC_{FF} for most of the time of the day during winter (Fig. 3c). This seems unlikely, when considering that it is not common that the houses are heated by burning wood during the whole course of the day nor does it seem likely that the BC_{WB} exceeds BC_{FF} substantially even during the evening. However, the highest α_{WB} values in the range 1.9–2.2 seem to be underestimating the contribution of BC_{WB} (Fig. 3c), if assuming that wood combustion is the major source of eBC at the residential site during evening. Zotter et al. (2017) comprehensively evaluated the site specific α values in Switzerland and observed α_{WB} values to typically vary in the range of 1.55–1.93. According to that study, lower α_{WB} values are recommended to be used in future studies for better estimating the BC_{WB} and BC_{FF} concentrations (Zotter et al., 2017). Based on the available information, we chose to use α_{WB} = 1.6 as a compromise for both locations. This is a slightly lower value than the commonly used α_{WB} values in the literature (Sandradewi et al., 2008b; Herich et al., 2011; Martinsson et al., 2017), however, considering the observations by Zotter et al. (2017), it is suitable approximation for the time being and leads to a reasonable daily cycle of the eBC components.

Nevertheless, it is important to highlight that there is a relatively large uncertainty in this estimation method. Overall, the uncertainty of the Aethalometer model source apportionment has been estimated to be in the level of 35% (Healy et al., 2017). In our study, the uncertainty can be even higher, since the eBC results were obtained from a PM_1 inlet, whereas levoglucosan was measured in PM_{10} samples and the sampling did not cover full seasonality at DH1. However, the difference in size fractions is presumably not dramatic, since levoglucosan is dominantly detected in PM_1 particles (Sillanpää et al., 2005; Engling et al., 2006; Saarikoski et al., 2008b; Frey et al., 2009). Furthermore, we acknowledge that the specificity of levoglucosan being a quantitative tracer for biomass burning and its stability in the atmosphere are disputable (Saarikoski et al., 2008a; Hennigan et al., 2010). Therefore, in lack of additional reference measurements, specifically those utilizing ^{14}C, we consider our approximation to be fit-for-purpose. This is valid based on the previous studies utilizing the similar estimation approach (Fuller et al., 2014; Titos et al., 2017).

As a summary, the estimated site specific α values were as follows: SC α_{FF} = 1.10 and α_{WB} = 1.60 and DH1 α_{FF} = 0.95 and α_{WB} = 1.60. Levoglucosan measurements were not conducted at the other detached house area site (DH2), therefore, we decided to use the same α combination as at DH1. This approximation is supported by the similar pattern of α values observed at both of these sites (Fig. S6), and by the similar characteristics of these sampling sites. Both α histograms from the detached house areas showed similar profiles and frequency peaking at higher α values when compared to the street canyon site (Fig. S6). The average BC_{WB} and BC_{FF} concentration levels shown in Table 1 were derived by using these optimized α value pairs.

3.3. Seasonal variation of BC_{FF} and BC_{WB}

The concentrations of BC_{FF} and BC_{WB} were calculated by using the site specific α values described above. The concentration levels and seasonal variations of BC_{WB} and BC_{FF} at the SC and DH1 sites were distinctly different (Fig. 4; Table 1). At DH1, both BC_{WB} and BC_{FF} concentrations decreased towards summer. Similarly, at SC the BC_{WB} concentrations somewhat decreased towards the summer, however, the BC_{FF} did not show a distinct seasonal dependency. The decrease in BC_{WB} concentrations during the warmer season at both sites is likely explained by the decrease in local and/or regional emissions from domestic heating by burning wood. This evidently affects the BC_{WB} concentration levels especially at the DH1 site, wherein the wood burning emissions are dominated by local appliances during winter. During winter, the BC_{WB} concentrations were on average 730 ± 1450 ng/m^3 and 180 ± 270 ng/m^3 at DH1 and SC, respectively. Focusing on the year 2016, a negative correlation was observed between air temperature with BC_{WB} at both DH1 (R = −0.54) and SC (R = −0.33), and with BC_{FF} at DH1 (R = −0.50). The seasonal pattern of BC_{WB}

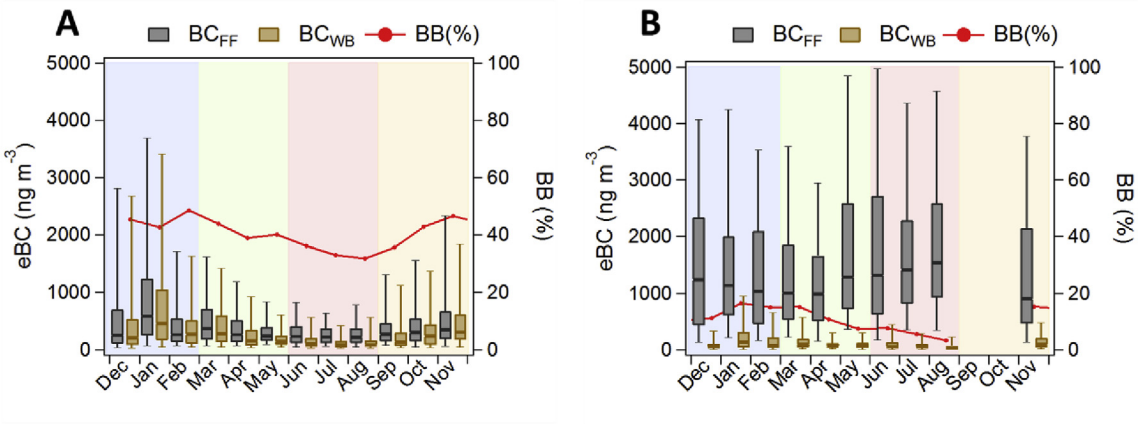

Fig. 4. Seasonal variation of BC_{FF} and BC_{WB} concentrations at a) detached house area 1 and b) street canyon during December 2015–November 2016. The shaded background colors are illustrative of seasons. The box and whisker plots represent 25th to 75th and 95th percentiles, respectively. The bold horizontal line shows the median. The biomass burning percentage (BB%) monthly median are shown on the right y-axis. (For interpretation of the references to color in this figure legend, the reader is referred to the Web version of this article.)

concentration followed those of other wood burning tracers, e.g. levoglucosan and benzo[*a*]pyrene, previously observed at the HMA (Saarnio et al., 2012; Hellén et al., 2017). Similar seasonal pattern of BC_{WB} has also been observed at other European locations (Herich et al., 2011; Fuller et al., 2014; Diapouli et al., 2017; Martinsson et al., 2017). In general, these results together with previous studies conducted in Finland (Hyvärinen et al., 2011; Saarnio et al., 2012), indicate that the seasonal trends of BC_{WB} and BC_{FF} can be expected to be quite similar in areas where traffic is low and wood burning sources are predominantly local.

Overall, the relative contribution of BC_{WB} to eBC (i.e. BB%) was higher at the DH1 site than at the SC site (Fig. 4 and Table 1). At DH1, the BB% was on average 46 ± 13% and 35 ± 13% during winter and summer, respectively. Similarly, at SC the contribution of BC_{WB} to eBC was higher during winter (17 ± 14%) than in summer (9 ± 10%). This difference between the seasons is typically observed at other locations as well due to the changes in wood burning emissions and meteorological conditions (Herich et al., 2011; Fuller et al., 2014; Becerril-Valle et al., 2017; Diapouli et al., 2017; Martinsson et al., 2017). On average, the BB% was similar at SC as in other urban locations in Europe, whereas the BB% at DH1 was typically slightly higher compared to other urban and rural locations (Table S3). Opposite to many other European countries, during the summer season, it is common in Finland to burn wood in sauna stoves and during outdoor activities (e.g. hot tubs, bonfires etc.). This, together with the low traffic volumes, may explain the relatively high BB% observed at the detached house area during summer. During summer at the SC site, the behavior is different. The regional BC_{WB} levels decrease from winter season, whereas the traffic volumes remain similar, which can be seen in the evident decrease of BB% (Fig. 4). Nevertheless, it cannot be excluded that the source apportionment may be partially failing at the DH1 during summer due to the overall low eBC concentration levels, due to varying α_{WB} values between seasons, or both.

As already mentioned, at the SC site, the BC_{FF} concentration levels were relatively constant throughout the year, although a slight increase could be seen during the summer season in 2016 (Fig. 4). This might be related to slightly changed traffic emissions due to tourist season, including increased emissions from both busses and cruise ships. However, it is not certain whether this represents a typical annual profile of BC_{FF} concentrations at the SC site. During early June, there was a tram-track maintenance job going on in the vicinity of SC site, which may have increased the nearby eBC emissions. However, even though the emissions from the nearby maintenance site may have increased the BC_{FF} concentration levels slightly during June, the BC_{FF} levels stayed relatively constant throughout the summer season (Fig. 4). Similar increase during summer has been previously observed at several locations in Ontario, Canada, wherein the increase was speculated to be due to difference in fuel summer/winter type, increased traffic rates and some other unidentified factor (Healy et al., 2017). The difference in fuel type may be a common factor between these studies. Previous studies covering eBC concentrations in Finland and in the HMA have typically observed low concentration levels during summer and high during winter (Järvi et al., 2008; Hyvärinen et al., 2011), similar to what was observed at the DH1 site in this study. Longer BC monitoring trends at the SC site are still needed to obtain more detailed understanding on the impacts of emission levels and meteorological conditions on seasonal BC_{FF} concentration patterns.

3.4. Diurnal variation of BC_{FF} and BC_{WB}

As depicted in Fig. 3, the diurnal profiles of BC_{WB} and BC_{FF} from winter and summer seasons at the SC and DH1 sites were clearly different. The corresponding diurnal cycles plotted by using the optimal α value combinations are presented in Fig. S7. Whereas the overall eBC diurnal profile at SC was bimodal, dominated by the morning and afternoon traffic peaks, the diurnal profile at DH1 showed increase towards the evening. The increasing eBC abundance towards the evening at DH1 might be influenced by both the residential heating (BC_{WB}) and the homecoming traffic (BC_{FF}) overlapping gradually. The contribution of BC_{WB} increases towards the evening at both sites, however, at DH1 the increase was more evident than at SC (Fig. S7). The observed diurnal cycles of BC_{WB} corroborate previous observations in other urban and rural locations (Fuller et al., 2014; Crilley et al., 2015; Diapouli et al., 2017; Martinsson et al., 2017; Titos et al., 2017).

The diurnal cycles of BC_{FF} observed at SC corroborate with previous studies conducted at sites influenced by traffic emissions (Herich et al., 2011; Fuller et al., 2014; Crilley et al., 2015; Jereb et al., 2018; Resquin et al., 2018). The diurnal cycle of BC_{FF} at SC bared close resemblance to the profile of NO_x concentration (Figs. S7 and S8), and overall the correlation between BC_{FF} with NO_x was significant during both summer ($R = 0.91$) and winter ($R = 0.94$) seasons. Oppositely, the correlation between NO_x with BC_{WB} was weaker during both winter ($R = 0.27$) and summer ($R = 0.32$). These observations are similar to previous studies (Herich et al., 2011; Crilley et al., 2015; Diapouli et al., 2017). During summer the BC_{FF} afternoon peak was relatively lower when compared to winter likely due to the difference in mixing layer height and stronger turbulent mixing (Järvi et al., 2008).

At the SC site, there was a difference in BC_{FF} diurnal cycles between weekdays and weekend (Fig. 5), similarly to the eBC diurnal cycles observed previously at HMA (Järvi et al., 2008), and at other traffic

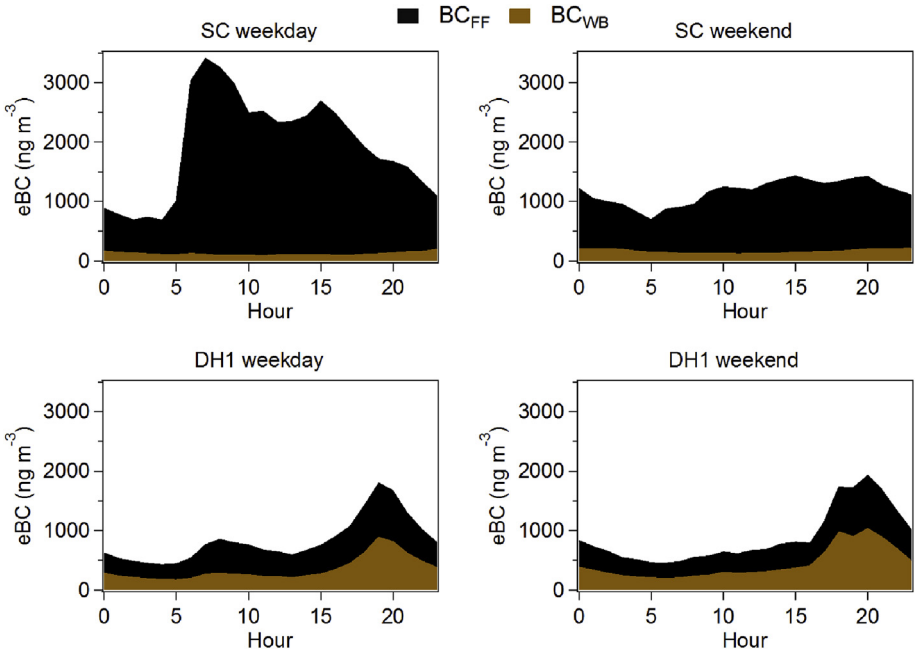

Fig. 5. Hourly averaged diurnal cycles of BC_{FF} and BC_{WB} concentrations at the street canyon (SC) and detached house area 1 (DH1) during weekdays and weekends in year 2016.

influenced sites (Herich et al., 2011; Reche et al., 2011; Fuller et al., 2014; Becerril-Valle et al., 2017; Zotter et al., 2017). The morning BC_{FF} traffic peak characteristic for weekdays was absent during weekend, and overall the concentration levels of BC_{FF} were lower during weekend (990 ± 770 ng/m^3) than in weekdays (1800 ± 1510 ng/m^3). This clearly demonstrates the effect of the nearby traffic on BC_{FF} levels at this site. The BC_{WB} diurnal cycles were similar during both weekend and weekday (Fig. 5), however, the concentration levels were slightly higher during weekend (160 ± 200 ng/m^3) than during weekdays (120 ± 200 ng/m^3).

At DH1, the diurnal cycles of BC_{FF} and BC_{WB} were relatively similar during both weekdays and weekend (Fig. 5). Only a small peak observed in BC_{FF} during morning traffic during weekdays was not present during the weekend. The average BC_{FF} concentrations were similar during both weekdays (490 ± 750 ng/m^3) and weekend (450 ± 720 ng/m^3), whereas the BC_{WB} concentrations were slightly higher during weekend (440 ± 900 ng/m^3) as compared to weekdays (350 ± 680 ng/m^3). In Finland, sauna stoves are extensively heated during Saturday, which likely explains the small increase in BC_{WB} levels. This is corroborated by previous studies covering biomass burning tracers that observed an increase during weekend as well (Saarikoski et al., 2008a; Saarnio et al., 2010, 2012; Hellén et al., 2017). In addition, similar difference in the diurnal cycles between weekdays and weekends was observed at the other detached house area (DH2, Fig. S9).

3.5. Source regions of BC_{FF} and BC_{WB}

Potential source areas of BC_{FF} and BC_{WB} were investigated by means of the bivariate polar plots (Fig. 6). The plots revealed some interesting features. At SC, the highest BC_{FF} levels were typically observed at low wind speeds (R = −0.42; Fig. 6), which indicates that the sources are likely local (Crilley et al., 2015), considering also the findings presented earlier. Oppositely, the highest BC_{WB} levels were observed at high wind speeds (Fig. 6), indicating distant regional sources (Crilley et al., 2015), although no statistically significant correlation was observed between wind speed with BC_{WB} concentration. Similar trends have been observed at sites, wherein the local and regional sources of eBC components are apparently different (Healy et al., 2017; Resquin et al., 2018). The BC_{FF} polar plots were somewhat similar during both summer and winter (Fig. S10), indicating the dominance of local sources, namely the close-by traffic emissions. However, the BC_{WB} showed somewhat different behavior (Fig. S10). The highest concentration levels were observed at varying wind speeds and directions during winter and summer. Consequently, due to the overall low BC_{WB} concentration levels, it is likely that even single long-range transport episodes and distant sources contribute to the observed patterns. Air masses arriving to southern Finland from Eastern Europe have been observed to elevate PM and BC concentration levels (Saarikoski et al., 2008a; Niemi et al., 2009).

At DH1, the BC_{WB} and BC_{FF} polar plots were remarkably similar, showing the highest concentration levels at low wind speeds (Fig. 6). The correlation between wind speed with BC_{WB} (R = −0.32) and BC_{FF} (R = −0.43) were moderate throughout the year. During winter, the highest BC_{WB} and BC_{FF} concentration levels were evidently observed at low wind speeds, whereas during summer, the highest concentrations were observed at slightly variable wind speeds coming from the east (Fig. S11). Thus, these results from DH1 suggest that during winter the local emissions are dominating, whereas during summer, the impact of local sources decreases. The wind direction sector containing the highest BC_{WB} and BC_{FF} concentration levels during summer is concurrent with the direction of the densely populated HMA urban district. Therefore, it is likely that during summer the eBC sources are more mixed and influenced by regional and distant sources in addition to local wood burning emissions from e.g. sauna stoves.

Recent studies have indicated that the filter-loading effect compensation parameter (k) used to correct the eBC results in real-time may be used as a proxy to differentiate some properties of the aerosol particles (Drinovec et al., 2015, 2017; Virkkula et al., 2015). Specifically, high values of k are considered to be indicative of local and freshly emitted particles, whereas low k values indicate ageing and coating during long-range transport (Drinovec et al., 2017). Even though the k parameter is not the main object of this study, we examined the variation of k at wavelength 880 nm (k_6) by following the procedure described in Drinovec et al. (2017). The k_6 values were higher during winter at DH1 (0.007 ± 0.001) than at SC (0.005 ± 0.001), whereas during summer the k_6 values were somewhat lower at DH1 (0.002 ± 0.002) than at SC (0.003 ± 0.002). The annual profile

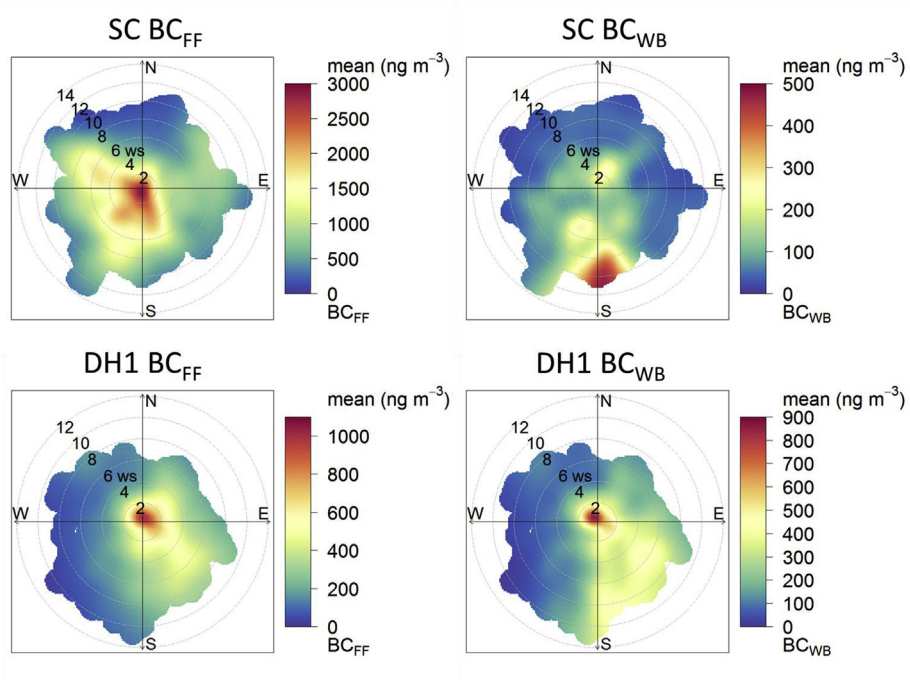

Fig. 6. Bivariate polar plots of BC_{FF} and BC_{WB} average concentrations at the street canyon (SC) and detached house area 1 (DH1) during 2016. The color scale indicates the average concentration levels and intervals the wind speed (ws, m/s). (For interpretation of the references to color in this figure legend, the reader is referred to the Web version of this article.)

showed significantly higher variation during the summer season at both locations when compared to winter (Fig. S12). In general, the seasonal trend was similar to previous observations in Finland and other locations (Virkkula et al., 2007; Drinovec et al., 2017). These k_6 observations, together with the α values (Fig. 1), indicate the dominance of local emission sources during the cold season (Drinovec et al., 2017). The large variation of k_6 values during summer (Fig. S12) suggests the contribution of distant sources and changes in particle coating and ageing processes. During spring and summer, changing meteorological conditions and an increase in biological activity increase the emissions from biogenic sources, including particles and gaseous compounds (Hakola et al., 2012). Among other pollutants, these factors contribute to the coating of particles during warm season, which potentially explains the observed variation of k_6 values. Nonetheless, the applicability of k_6 being an adequate proxy for these properties requires further evaluation.

3.6. Contribution of eBC, BC_{FF} and BC_{WB} to $PM_{2.5}$

Overall, the contribution of eBC (in PM_1) to $PM_{2.5}$ was on average somewhat higher at SC (21 ± 17%) than at DH1 (14 ± 18%) during the year 2016. In general, these results are in line with previously observed eBC/PM-ratios at HMA and at other locations (Pakkanen et al., 2000; Reche et al., 2011; Aurela et al., 2015; Elser et al., 2016; Becerril-Valle et al., 2017), although the difference in size fractions somewhat hinders the comparability. The portion of BC_{FF} to $PM_{2.5}$ was evidently higher at SC than at DH1 during winter and especially during summer (Table 2). Oppositely, the relative amount of BC_{WB} to $PM_{2.5}$ was higher at DH1 than at SC during winter, whereas during summer the contribution was relatively similar at both sites (Table 2).

Table 2
The relative amount of eBC, BC_{FF} and BC_{WB} to $PM_{2.5}$ at the street canyon (SC) and detached house area 1 (DH1) during different seasons.

Season	Fraction	SC	DH1
Winter	eBC/$PM_{2.5}$	21 ± 18%	18 ± 20%
	$BC_{WB}/PM_{2.5}$	2 ± 7%	9 ± 13%
	$BC_{FF}/PM_{2.5}$	19 ± 18%	11 ± 15%
Summer	eBC/$PM_{2.5}$	25 ± 19%	9 ± 16%
	$BC_{WB}/PM_{2.5}$	2 ± 5%	4 ± 11%
	$BC_{FF}/PM_{2.5}$	24 ± 19%	7 ± 14%

At the DH1 site, the contribution of BC_{FF} and BC_{WB} to $PM_{2.5}$ was larger in winter than in summer. The seasonal difference is likely due to decline in wood burning emissions, meteorological conditions and the influence of increasing contribution of secondary organic aerosol formation during summer (Saarikoski et al., 2008a; Reche et al., 2011; Becerril-Valle et al., 2017). The diurnal pattern of $PM_{2.5}$ (Fig. S8) had similar features to the patterns of BC_{FF} and BC_{WB} during both summer and winter at DH1 (Fig. S7), namely the increase in concentration levels towards the evening and night. The correlation between $PM_{2.5}$ with BC_{WB} (R = 0.86) and BC_{FF} (R = 0.87) were similar during winter, whereas during summer the correlation was stronger with BC_{FF} (R = 0.81) than with BC_{WB} (R = 0.69). Consequently, eBC and PM are likely to have similar sources at this site, the most evident one being wood combustion during winter, regional sources and long-range transport.

Interestingly, the contribution of BC_{FF} to $PM_{2.5}$ did not decrease during summer at SC. This could indicate, that traffic emissions are a rather constant source of PM and eBC at this site. However, during winter the correlation was stronger between $PM_{2.5}$ with BC_{WB} (R = 0.83) than with BC_{FF} (R = 0.54). An opposite situation was observed during summer, when the correlation was stronger between $PM_{2.5}$ with BC_{FF} (R = 0.57) than with BC_{WB} (R = 0.39). The diurnal cycle of $PM_{2.5}$ showed the characteristic BC_{FF} morning traffic peak during summer (Fig. S8), whereas during winter the diurnal cycle of $PM_{2.5}$ was slightly peaking during the afternoon and was not particularly resembling either BC_{FF} or BC_{WB} diurnal cycles (Fig. S7). This discrepancy might be because PM sources are not solely reflected by traffic emissions at this site, whereas eBC is likely dominantly influenced by the local traffic sources. This phenomenon has also been previously addressed at other traffic dominant sites (Reche et al., 2011).

4. Conclusions

The results from this study demonstrate the large variability in temporal and spatial eBC sources within the Helsinki metropolitan area, being closely tied to the characteristics of the measurement site, season, meteorological conditions and the time of the day. On average, the eBC

concentrations were larger at the street canyon site than at the detached house areas. The eBC concentrations were dominated by traffic emissions at the street canyon site, whereas the largest concentrations of eBC observed at the detached house areas were attributed to being influenced by wood combustion due to residential heating and warming of sauna stoves.

The impact of fossil fuel and wood burning emissions on the measured eBC concentrations were estimated by determining separate α_{FF} and α_{WB} values for the street canyon and detached house area sites. In principle, the source apportionment method performed better at the street canyon site where the BC_{FF} and BC_{WB} were clearly separated. For the detached house area, it is possible that the determined α_{FF} and α_{WB} values were not entirely representative, since the separation of BC_{FF} and BC_{WB} was not always obvious. eBC sources were substantially mixed in the detached house area, which made it more difficult to reliably separate the BC_{FF} and BC_{WB} components. Thus, an additional analysis of aerosol chemical composition (e.g. ^{14}C analysis) at detached house area would be beneficial for eBC sources apportionment. Furthermore, additional measurements of the direct emissions from e.g. sauna stove and masonry heaters with an aethalometer could provide valuable information for the selection of α_{WB} value in the Aethalometer model.

This study clearly revealed the differences in the sources of eBC in the street canyon and detached house area sites in the Helsinki metropolitan area. Especially the impact of wood burning on eBC concentrations gives valuable information that has been previously missing. It is noteworthy, that during cold winter periods the eBC concentration levels were similar at the street canyon site and at the detached house areas, demonstrating the impact, magnitude and regional dispersion of wood burning emissions. The knowledge of the sources of eBC in urban and suburban areas will provide tools for improving the decision making, e.g. city planning and relevant source emission restrictions. The better knowledge of the sources of ambient particles and/or specific species can be used to improve the emission legislation and to assess how air quality could be improved. Especially important would be to estimate what are the most cost effective means to reduce air pollution, and evaluate the effect of combustion emissions on climate change. Considering the previous and current technology advancement in engines and exhaust after-treatment systems, it can be expected that the BC_{FF} emissions are declining in the future. However, wood burning emissions are not explicitly restricted and the replacement of current residential wood burning technology (masonry heaters and sauna stoves) is not taking place in near future.

Acknowledgements

This study has been funded by TEKES funded INKA-ILMA/EAKR project (Tekes project no. 4588/31/2015, industrial partners: Dekati Oy, Genano Oy, Nordic Envicon Oy, Pegasor Oy, Sandbox Oy, Suomen Terveysilma Oy, TreLab Oy, Vallox Oy) and by the Regional innovations and experimentations funds AIKO, governed by the Helsinki Regional Council (project HAQT, AIKO014). Long-term research cooperation and financial support from HSY to this project is gratefully acknowledged.

Appendix A. Supplementary data

Supplementary data related to this article can be found at https://doi.org/10.1016/j.atmosenv.2018.07.022.

References

Andreae, M., Gelencsér, A., 2006. Black carbon or brown carbon? The nature of light-absorbing carbonaceous aerosols. Atmos. Chem. Phys. 6, 3131–3148.
Aurela, M., Saarikoski, S., Niemi, J.V., Canonaco, F., Prevot, A.S., Frey, A., Carbone, S., Kousa, A., Hillamo, R., 2015. Chemical and source characterization of submicron particles at residential and traffic sites in the Helsinki Metropolitan area, Finland. Aerosol Air Qual. Res. 15, 1213–1226.
Becerril-Valle, M., Coz, E., Prévôt, A., Močnik, G., Pandis, S., de la Campa, A.S., Alastuey, A., Díaz, E., Pérez, R., Artíñano, B., 2017. Characterization of atmospheric black carbon and co-pollutants in urban and rural areas of Spain. Atmos. Environ. 169, 36–53.
Birmili, W., Weinhold, K., Rasch, F., Sonntag, A., Sun, J., Merkel, M., Wiedensohler, A., Bastian, S., Schladitz, A., Löschau, G., 2016. Long-term observations of tropospheric particle number size distributions and equivalent black carbon mass concentrations in the German Ultrafine Aerosol Network (GUAN). Earth Syst. Sci. Data 8, 355–382.
Bond, T.C., Doherty, S.J., Fahey, D., Forster, P., Berntsen, T., DeAngelo, B., Flanner, M., Ghan, S., Kärcher, B., Koch, D., 2013. Bounding the role of black carbon in the climate system: a scientific assessment. J. Geophys. Res. Atmos. 118, 5380–5552.
Briggs, N.L., Long, C.M., 2016. Critical review of black carbon and elemental carbon source apportionment in Europe and the United States. Atmos. Environ. 144, 409–427.
Carslaw, D.C., Beevers, S.D., 2013. Characterising and understanding emission sources using bivariate polar plots and k-means clustering. Environ. Model. Software 40, 325–329.
Carslaw, D.C., Ropkins, K., 2012. Openair—an R package for air quality data analysis. Environ. Model. Software 27, 52–61.
Carslaw, D., Ropkins, K., 2017. Openair: Open-source Tools for the Analysis of Air Pollution Data, R Package Version 2.1-5. 2017 available at: https://CRAN.R-project.org/package=openair, Accessed date: 20 November 2017.
Cavalli, F., Viana, M., Yttri, K.E., Genberg, J., Putaud, J.-P., 2010. Toward a standardised thermal-optical protocol for measuring atmospheric organic and elemental carbon: the EUSAAR protocol. Atmos. Meas. Tech 3, 79–89.
Crilley, L.R., Bloss, W.J., Yin, J., Beddows, D.C.S., Harrison, R.M., Allan, J.D., Young, D.E., Flynn, M., Williams, P., Zotter, P., Prevot, A.S.H., Heal, M.R., Barlow, J.F., Halios, C.H., Lee, J.D., Szidat, S., Mohr, C., 2015. Sources and contributions of wood smoke during winter in London: assessing local and regional influences. Atmos. Chem. Phys. 15, 3149–3171.
Diapouli, E., Kalogridis, A.-C., Markantonaki, C., Vratolis, S., Fetfatzis, P., Colombi, C., Eleftheriadis, K., 2017. Annual variability of black carbon concentrations originating from biomass and fossil fuel combustion for the suburban aerosol in Athens, Greece. Atmosphere 8, 234.
Drinovec, L., Močnik, G., Zotter, P., Prévôt, A., Ruckstuhl, C., Coz, E., Rupakheti, M., Sciare, J., Müller, T., Wiedensohler, A., 2015. The" dual-spot" Aethalometer: an improved measurement of aerosol black carbon with real-time loading compensation. Atmos. Meas. Tech 8, 1965–1979.
Drinovec, L., Gregoric, A., Zotter, P., Wolf, R., Bruns, E.A., Prévôt, A.S., Petit, J.-E., Favez, O., Sciare, J., Arnold, I.J., 2017. The filter-loading effect by ambient aerosols in filter absorption photometers depends on the coating of the sampled particles. Atmos. Meas. Tech 10, 1043–1059.
Elser, M., Bozzetti, C., El-Haddad, I., Maasikmets, M., Teinemaa, E., Richter, R., Wolf, R., Slowik, J.G., Baltensperger, U., Prévôt, A.S., 2016. Urban increments of gaseous and aerosol pollutants and their sources using mobile aerosol mass spectrometry measurements. Atmos. Chem. Phys. 16, 7117–7134.
Engling, G., Carrico, C.M., Kreidenweis, S.M., Collett, J.L., Day, D.E., Malm, W.C., Lincoln, E., Hao, W.M., Iinuma, Y., Herrmann, H., 2006. Determination of levoglucosan in biomass combustion aerosol by high-performance anion-exchange chromatography with pulsed amperometric detection. Atmos. Environ. 40, 299–311.
Enroth, J., Saarikoski, S., Niemi, J., Kousa, A., Ježek, I., Močnik, G., Carbone, S., Kuuluvainen, H., Rönkkö, T., Hillamo, R., Pirjola, L., 2016. Chemical and physical characterization of traffic particles in four different highway environments in the Helsinki metropolitan area. Atmos. Chem. Phys. 16, 5497–5512.
Frey, A.K., Tissari, J., Saarnio, K.M., Timonen, H.J., Tolonen-Kivimäki, O., Aurela, M.A., Saarikoski, S.K., Makkonen, U., Hytönen, K., Jokiniemi, J., 2009. Chemical composition and mass size distribution of fine particulate matter emitted by a small masonry heater. Boreal Environ. Res. 14, 255–271.
Fuller, G.W., Tremper, A.H., Baker, T.D., Yttri, K.E., Butterfield, D., 2014. Contribution of wood burning to PM 10 in London. Atmos. Environ. 87, 87–94.
Garg, S., Chandra, B.P., Sinha, V., Sarda-Esteve, R., Gros, V., Sinha, B., 2015. Limitation of the use of the absorption angstrom exponent for source apportionment of equivalent black carbon: a case study from the north west indo-gangetic plain. Environ. Sci. Technol. 50, 814–824.
Gyawali, M., Arnott, W., Lewis, K., Moosmüller, H., 2009. In situ aerosol optics in Reno, NV, USA during and after the summer 2008 California wildfires and the influence of absorbing and non-absorbing organic coatings on spectral light absorption. Atmos. Chem. Phys. 9, 8007–8015.
Hakola, H., Hellén, H., Hemmilä, M., Rinne, J., Kulmala, M., 2012. In situ measurements of volatile organic compounds in a boreal forest. Atmos. Chem. Phys. 12, 11665–11678.
Hansen, J., Nazarenko, L., 2004. Soot climate forcing via snow and ice albedos. P. Natl. Acad. Sci. USA 101, 423–428.
Hansen, A., Rosen, H., Novakov, T., 1984. The aethalometer—an instrument for the real-time measurement of optical absorption by aerosol particles. Sci. Total Environ. 36, 191–196.
Harrison, R.M., Beddows, D.C., Jones, A.M., Calvo, A., Alves, C., Pio, C., 2013. An evaluation of some issues regarding the use of aethalometers to measure woodsmoke concentrations. Atmos. Environ. 80, 540–548.
Healy, R., Sofowote, U., Su, Y., Debosz, J., Noble, M., Jeong, C.-H., Wang, J., Hilker, N., Evans, G., Doerksen, G., 2017. Ambient measurements and source apportionment of fossil fuel and biomass burning black carbon in Ontario. Atmos. Environ. 161, 34–47.
Hellén, H., Kangas, L., Kousa, A., Vestenius, M., Teinilä, K., Karppinen, A., Kukkonen, J., Niemi, J.V., 2017. Evaluation of the impact of wood combustion on benzo [a] pyrene (BaP) concentrations; ambient measurements and dispersion modeling in Helsinki, Finland. Atmos. Chem. Phys. 17, 3475–3487.

Hennigan, C.J., Sullivan, A.P., Collett, J.L., Robinson, A.L., 2010. Levoglucosan stability in biomass burning particles exposed to hydroxyl radicals. Geophys. Res. Lett. 37, L09806.
Herich, H., Hueglin, C., Buchmann, B., 2011. A 2.5 year's source apportionment study of black carbon from wood burning and fossil fuel combustion at urban and rural sites in Switzerland. Atmos. Meas. Tech 4, 1409–1420.
Hienola, A., Pietikäinen, J.-P., Jacob, D., Pozdun, R., Petäjä, T., Hyvärinen, A.-P., Sogacheva, L., Kerminen, V.-M., Kulmala, M., Laaksonen, A., 2013. Black carbon concentration and deposition estimations in Finland by the regional aerosol-climate model REMO-HAM. Atmos. Chem. Phys. 13, 4033–4055.
Hyvärinen, A.-P., Kolmonen, P., Kerminen, V.-M., Virkkula, A., Leskinen, A., Komppula, M., Hatakka, J., Burkhart, J., Stohl, A., Aalto, P., 2011. Aerosol black carbon at five background measurement sites over Finland, a gateway to the Arctic. Atmos. Environ. 45, 4042–4050.
IPCC, 2014. In: Pachauri, R.K., Meyer, L.A. (Eds.), Climate Change 2014: Synthesis Report. Contribution of Working Groups I, II and III to the Fifth Assessment Report of the Intergovernmental Panel on Climate Change [Core Writing Team, Geneva, Switzerland, 151 pp.
Järvi, L., Junninen, H., Karppinen, A., Hillamo, R., Virkkula, A., Mäkelä, T., Pakkanen, T., Kulmala, M., 2008. Temporal variations in black carbon concentrations with different time scales in Helsinki during 1996–2005. Atmos. Chem. Phys. 8, 1017–1027.
Jereb, B., Batkovič, T., Herman, L., Šipek, G., Kovše, Š., Gregorič, A., Močnik, G., 2018. Exposure to black carbon during bicycle commuting–alternative route selection. Atmosphere 9, 21.
Kaski, N., Loukkola, K., Portin, H., 2017. Air Quality in the Helsinki Metropolitan Area in 2016. HSY publications.
Kirchstetter, T.W., Novakov, T., Hobbs, P.V., 2004. Evidence that the spectral dependence of light absorption by aerosols is affected by organic carbon. J. Geophys. Res. Atmos. 109.
Klimont, Z., Kupiainen, K., Heyes, C., Purohit, P., Cofala, J., Rafaj, P., Borken-Kleefeld, J., Schöpp, W., 2017. Global anthropogenic emissions of particulate matter including black carbon. Atmos. Chem. Phys. 17, 8681–8723.
Lack, D., Cappa, C., 2010. Impact of brown and clear carbon on light absorption enhancement, single scatter albedo and absorption wavelength dependence of black carbon. Atmos. Chem. Phys. 10, 4207–4220.
Lack, D., Langridge, J., 2013. On the attribution of black and brown carbon light absorption using the Ångström exponent. Atmos. Chem. Phys. 13, 10535–10543.
Laskin, A., Laskin, J., Nizkorodov, S.A., 2015. Chemistry of atmospheric brown carbon. Chem. Rev. 115, 4335–4382.
Liu, D., Allan, J.D., Young, D.E., Coe, H., Beddows, D., Fleming, Z.L., Flynn, M.J., Gallagher, M.W., Harrison, R.M., Lee, J., Prevot, A.S.H., Taylor, J.W., Yin, J., Williams, P.I., Zotter, P., 2014. Size distribution, mixing state and source apportionment of black carbon aerosol in London during wintertime. Atmos. Chem. Phys. 14, 10061–10084.
Magee Scientific, 2016. Aethalometer® Model AE33 User Manual Version 1.54. Magee Scientific.
Martinsson, J., Eriksson, A., Nielsen, I.E., Malmborg, V.B., Ahlberg, E., Andersen, C., Lindgren, R., Nystrom, R., Nordin, E., Brune, W., 2015. Impacts of combustion conditions and photochemical processing on the light absorption of biomass combustion aerosol. Environ. Sci. Technol. 49, 14663–14671.
Martinsson, J., Abdul Azeem, H., Sporre, M.K., Bergström, R., Ahlberg, E., Öström, E., Kristensson, A., Swietlicki, E., Eriksson Stenström, K., 2017. Carbonaceous aerosol source apportionment using the Aethalometer model–evaluation by radiocarbon and levoglucosan analysis at a rural background site in southern Sweden. Atmos. Chem. Phys. 17, 4265–4281.
Massoli, P., Fortner, E.C., Canagaratna, M.R., Williams, L.R., Zhang, Q., Sun, Y., Schwab, J.J., Trimborn, A., Onasch, T.B., Demerjian, K.L., 2012. Pollution gradients and chemical characterization of particulate matter from vehicular traffic near major roadways: results from the 2009 Queens College Air Quality Study in NYC. Aerosol Sci. Technol. 46, 1201–1218.
Niemi, J.V., Saarikoski, S., Aurela, M., Tervahattu, H., Hillamo, R., Westphal, D.L., Aarnio, P., Koskentalo, T., Makkonen, U., Vehkamäki, H., 2009. Long-range transport episodes of fine particles in southern Finland during 1999–2007. Atmos. Environ. 43, 1255–1264.
Pakkanen, T.A., Kerminen, V.-M., Ojanen, C.H., Hillamo, R.E., Aarnio, P., Koskentalo, T., 2000. Atmospheric black carbon in Helsinki. Atmos. Environ. 34, 1497–1506.
Petit, J.-E., Amodeo, T., Meleux, F., Bessagnet, B., Menut, L., Grenier, D., Pellan, Y., Ockler, A., Rocq, B., Gros, V., 2017. Characterising an intense PM pollution episode in March 2015 in France from multi-site approach and near real time data: climatology, variabilities, geographical origins and model evaluation. Atmos. Environ. 155, 68–84.
Petzold, A., Schönlinner, M., 2004. Multi-angle absorption photometry—a new method for the measurement of aerosol light absorption and atmospheric black carbon. J. Aerosol Sci. 35, 421–441.
Petzold, A., Ogren, J.A., Fiebig, M., Laj, P., Li, S.M., Baltensperger, U., Holzer-Popp, T., Kinne, S., Pappalardo, G., Sugimoto, N., Wehrli, C., Wiedensohler, A., Zhang, X.Y., 2013. Recommendations for reporting "black carbon" measurements. Atmos. Chem. Phys. 13, 8365–8379.
Pirjola, L., Niemi, J.V., Saarikoski, S., Aurela, M., Enroth, J., Carbone, S., Saarnio, K., Kuuluvainen, H., Kousa, A., Rönkkö, T., 2017. Physical and chemical characterization of urban winter-time aerosols by mobile measurements in Helsinki, Finland. Atmos. Environ. 158, 60–75.
Pöschl, U., 2003. Aerosol particle analysis: challenges and progress. Anal. Bioanal. Chem. 375, 30–32.
Puxbaum, H., Caseiro, A., Sánchez-Ochoa, A., Kasper-Giebl, A., Claeys, M., Gelencsér, A., Legrand, M., Preunkert, S., Pio, C., 2007. Levoglucosan levels at background sites in Europe for assessing the impact of biomass combustion on the European aerosol background. J. Geophys. Res. Atmos. 112, D23S05.
R Core Team, 2017. R: a Language and Environment for Statistical Computing. R Foundation for Statistical Computing, Vienna, Austria available at: https://www.r-project.org/, Accessed date: 20 November 2017.
Rajesh, T., Ramachandran, S., 2017. Characteristics and source apportionment of black carbon aerosols over an urban site. Environ. Sci. Pollut. Res. 24, 8411–8424.
Ran, L., Deng, Z., Wang, P., Xia, X., 2016. Black carbon and wavelength-dependent aerosol absorption in the North China Plain based on two-year aethalometer measurements. Atmos. Environ. 142, 132–144.
Reche, C., Querol, X., Alastuey, A., Viana, M., Pey, J., Moreno, T., Rodríguez, S., González, Y., Fernández-Camacho, R., Rosa, J.d.l, 2011. New considerations for PM, Black Carbon and particle number concentration for air quality monitoring across different European cities. Atmos. Chem. Phys. 11, 6207–6227.
Resquin, M.D., Santágata, D., Gallardo, L., Gómez, D., Rössler, C., Dawidowski, L., 2018. Local and remote black carbon sources in the metropolitan area of buenos Aires. Atmos. Environ. 182, 105–114.
Saarikoski, S., Timonen, H., Saarnio, K., Aurela, M., Järvi, L., Keronen, P., Kerminen, V.-M., Hillamo, R., 2008a. Sources of organic carbon in fine particulate matter in northern European urban air. Atmos. Chem. Phys. 8, 6281–6295.
Saarikoski, S.K., Sillanpää, M.K., Saarnio, K.M., Hillamo, R.E., Pennanen, A.S., Salonen, R.O., 2008b. Impact of biomass combustion on urban fine particulate matter in Central and Northern Europe. Water, Air, Soil Pollut. 191, 265–277.
Saarnio, K., Teinilä, K., Aurela, M., Timonen, H., Hillamo, R., 2010. High-performance anion-exchange chromatography–mass spectrometry method for determination of levoglucosan, mannosan, and galactosan in atmospheric fine particulate matter. Anal. Bioanal. Chem. 398, 2253–2264.
Saarnio, K., Niemi, J.V., Saarikoski, S., Aurela, M., Timonen, H., Teinilä, K., Myllynen, M., Freyi, A., Lamberg, H., Jokiniemi, J., 2012. Using monosaccharide anhydrides to estimate the impact of wood combustion on fine particles in the Helsinki Metropolitan Area. Boreal Environ. Res. 17, 163–183.
Saarnio, K., Teinilä, K., Saarikoski, S., Carbone, S., Gilardoni, S., Timonen, H., Aurela, M., Hillamo, R., 2013. Online determination of levoglucosan in ambient aerosols with particle-into-liquid sampler–high-performance anion-exchange chromatography–mass spectrometry (PILS–HPAEC–MS). Atmos. Meas. Tech 6, 2839–2849.
Saleh, R., Hennigan, C., McMeeking, G., Chuang, W., Robinson, E., Coe, H., Donahue, N., Robinson, A., 2013. Absorptivity of brown carbon in fresh and photo-chemically aged biomass-burning emissions. Atmos. Chem. Phys. 13, 7683–7693.
Sandradewi, J., Prévôt, A., Weingartner, E., Schmidhauser, R., Gysel, M., Baltensperger, U., 2008a. A study of wood burning and traffic aerosols in an Alpine valley using a multi-wavelength Aethalometer. Atmos. Environ. 42, 101–112.
Sandradewi, J., Prévôt, A.S., Szidat, S., Perron, N., Alfarra, M.R., Lanz, V.A., Weingartner, E., Baltensperger, U., 2008b. Using aerosol light absorption measurements for the quantitative determination of wood burning and traffic emission contributions to particulate matter. Environ. Sci. Technol. 42, 3316–3323.
Savolahti, M., Karvosenoja, N., Tissari, J., Kupiainen, K., Sippula, O., Jokiniemi, J., 2016. Black carbon and fine particle emissions in Finnish residential wood combustion: emission projections, reduction measures and the impact of combustion practices. Atmos. Environ. 140, 495–505.
Sciare, J., d'Argouges, O., Sarda-Estève, R., Gaimoz, C., Dolgorouky, C., Bonnaire, N., Favez, O., Bonsang, B., Gros, V., 2011. Large contribution of water-insoluble secondary organic aerosols in the region of Paris (France) during wintertime. J. Geophys. Res. Atmos. 116.
Sillanpää, M., Saarikoski, S., Hillamo, R., Pennanen, A., Makkonen, U., Spolnik, Z., Van Grieken, R., Koskentalo, T., Salonen, R.O., 2005. Chemical composition, mass size distribution and source analysis of long-range transported wildfire smokes in Helsinki. Sci. Total Environ. 350, 119–135.
Simoneit, B.R., Schauer, J.J., Nolte, C., Oros, D.R., Elias, V.O., Fraser, M., Rogge, W., Cass, G.R., 1999. Levoglucosan, a tracer for cellulose in biomass burning and atmospheric particles. Atmos. Environ. 33, 173–182.
Singh, V., Ravindra, K., Sahu, L., Sokhi, R., 2018. Trends of atmospheric black carbon concentration over United Kingdom. Atmos. Environ. 178, 148–157.
Tissari, J., Hytönen, K., Lyyränen, J., Jokiniemi, J., 2007. A novel field measurement method for determining fine particle and gas emissions from residential wood combustion. Atmos. Environ. 41, 8330–8344.
Titos, G., Del Águila, A., Cazorla, A., Lyamani, H., Casquero-Vera, J., Colombi, C., Cuccia, E., Gianelle, V., Močnik, G., Alastuey, A., 2017. Spatial and temporal variability of carbonaceous aerosols: assessing the impact of biomass burning in the urban environment. Sci. Total Environ. 578, 613–625.
Virkkula, A., Mäkelä, T., Hillamo, R., Yli-Tuomi, T., Hirsikko, A., Hämeri, K., Koponen, I.K., 2007. A simple procedure for correcting loading effects of aethalometer data. J. Air Waste Manage 57, 1214–1222.
Virkkula, A., Chi, X., Ding, A., Shen, Y., Nie, W., Qi, X., Zheng, L., Huang, X., Xie, Y., Wang, J., Petäjä, T., Kulmala, M., 2015. On the interpretation of the loading correction of the aethalometer. Atmos. Meas. Tech 8, 4415–4427.
Wang, Y., Hopke, P.K., Rattigan, O.V., Xia, X., Chalupa, D.C., Utell, M.J., 2011a. Characterization of residential wood combustion particles using the two-wavelength aethalometer. Environ. Sci. Technol. 45, 7387–7393.
Wang, Y., Hopke, P.K., Rattigan, O.V., Zhu, Y., 2011b. Characterization of ambient black carbon and wood burning particles in two urban areas. J. Environ. Monit. 13, 1919–1926.
WHO, 2012. Health Effects of Black Carbon. World Health Organization, Regional Office for Europe, Copenhagen.
Yttri, K.E., Dye, C., Slørdal, L.H., Braathen, O.-A., 2005. Quantification of monosaccharide anhydrides by liquid chromatography combined with mass spectrometry: application to aerosol samples from an urban and a suburban site influenced by

small-scale wood burning. J. Air Waste Manage 55, 1169–1177.
Zhu, Y., Hinds, W.C., Kim, S., Shen, S., Sioutas, C., 2002. Study of ultrafine particles near a major highway with heavy-duty diesel traffic. Atmos. Environ. 36, 4323–4335.
Zhu, C.-S., Cao, J.-J., Hu, T.-F., Shen, Z.-X., Tie, X.-X., Huang, H., Wang, Q.-Y., Huang, R.-J., Zhao, Z.-Z., Močnik, G., 2017. Spectral dependence of aerosol light absorption at an urban and a remote site over the. Tibetan Plateau. Sci. Total Environ 590, 14–21.
Zotter, P., Herich, H., Gysel, M., El-Haddad, I., Zhang, Y., Močnik, G., Hüglin, C., Baltensperger, U., Szidat, S., Prévôt, A.S.H., 2017. Evaluation of the absorption Ångström exponents for traffic and wood burning in the Aethalometer-based source apportionment using radiocarbon measurements of ambient aerosol. Atmos. Chem. Phys. 17, 4229–4249.